Int. J. Multiphase Flow Vol. 18, No. 6, pp. 821–830, 1992
Printed in Great Britain.

0301-9322/92 $5.00 + 0.00

STRUCTURAL AND INTERFACIAL STABILITY OF MULTIPLE SOLUTIONS FOR STRATIFIED FLOW

D. BARNEA and Y. TAITEL

Department of Fluid Mechanics and Heat Transfer, Faculty of Engineering, Tel-Aviv University, Ramat-Aviv, Tel-Aviv 69978, Israel

(Received 9 February 1992; in revised form 25 August 1992)

Abstract—Prediction of the liquid level in stratified two-phase upwards flow shows that one may have multiple solutions. In this case it is necessary to determine which solutions will actually occur and whether hysteresis is possible, namely whether it is possible to have two or more solutions for the same operating conditions. In this work the stability of the solutions for stratified flow is considered using two types of stability analyses: (1) structural stability analysis; and (2) interfacial stability analysis (Kelvin–Helmholtz, K–H). For the K–H stability analysis we used two methods: an approximate simplified method suggested by Taitel & Dukler; and a more rigorous method suggested by Barnea, which is based on a combination of the viscous K–H and inviscid K–H analyses. The results show that whenever three solutions exist only the first, i.e. the solution with the thinnest liquid level, is stable. The middle solution is always structurally unstable (linearly), whereas the third solution is structurally unstable to large disturbances (non-linear stability). The third solution is usually also unstable to the K–H type of instability. As a result it is concluded that hysteresis is not possible and that only the thinnest solution will be observed practically.

Key Words: two-phase, stratified flow, stability, Kelvin–Helmholtz, flow pattern

INTRODUCTION

The prediction of the liquid level in stratified flow is the first step in analyzing the stability of stratified flow and for developing the transition criteria to either slug or annular flow. The transition criteria are based on the classical linear Kelvin–Helmholtz (K–H) stability analysis. Taitel & Dukler (1976) used a simplified K–H analysis and derived a criterion for the transition from stratified flow. Wallis (1969), Lin & Hanratty (1986) and Wu *et al.* (1987) included the effect of the shear stresses in their linear stability analyses (the viscous K–H analysis). Recently, Barnea (1991a) suggested a combined model which uses the viscous and inviscid K–H theories for the determination of the transition to slug and annular flow.

All the above stability analyses are performed on the equilibrium stratified flow solution. As pointed by Baker & Gravestock (1987), the solution for the steady-state liquid level is not unique and multiple solutions may occur for some operating conditions in upward inclined flow. In this case one may question whether multiple holdup values exist for stable stratified flow. Landman (1991a,b), who considered this question, suggested the existence of two possible physical solutions in the region of stratified flow.

A similar problem has been raised by Barnea & Taitel (1989) and Barnea (1991b) for the case of annular flow. They suggested that one should distinguish between the stability of the interface and the stability of the steady-state solution, where the solution is obtained for an average film thickness using an effective interfacial shear stress. A similar concept will be applied here to the case of stratified flow.

The first step in the present work is to perform a stability analysis that will determine which solution is physically stable with respect to its average film thickness (even if the interface is unstable due to the K–H instability). This analysis will be termed the "structural stability analysis". Only when the solution is structurally stable is the K–H stability analysis performed as a further check for the stability of stratified flow.

An alternative way to look at the problem is to perform the K–H analysis on the various solutions and then to check for the stability of the structure for those solutions that are in the region of stratified flow.

STRUCTURAL STABILITY

Structural linear stability

The analysis of stratified flow is based here on the "two-fluid model", where transient integral continuity and momentum equations are applied to the gas and the liquid, together with the appropriate "constitutive" relations. Assuming incompressible isothermal flow, neglecting surface tension effects and equating the pressure drop in the two phases yields the following three equations (Barnea 1991a):

$$\frac{\partial R_L}{\partial t} + R_L \frac{\partial U_L}{\partial x} + U_L \frac{\partial R_L}{\partial x} = 0, \quad [1]$$

$$\frac{\partial R_G}{\partial t} + R_G \frac{\partial U_G}{\partial x} + U_G \frac{\partial R_G}{\partial x} = 0, \quad [2]$$

and

$$\rho_L \frac{\partial U_L}{\partial t} - \rho_G \frac{\partial U_G}{\partial t} + \rho_L U_L \frac{\partial U_L}{\partial x} - \rho_G U_G \frac{\partial U_G}{\partial x} + (\rho_L - \rho_G) g \cos\beta \frac{A}{A'_L} \frac{\partial R_L}{\partial x} = F, \quad [3]$$

where

$$F = -\frac{\tau_L S_L}{A R_L} + \frac{\tau_G S_G}{A R_G} + \frac{\tau_i S_i}{A}\left(\frac{1}{R_L} + \frac{1}{R_G}\right) - (\rho_L - \rho_G) g \sin\beta, \quad [4]$$

A is the cross-sectional area, U is the axial average velocity, τ is the wall shear stress, τ_i is the interfacial shear stress, S and S_i are the perimeters over which τ and τ_i act, R is the phase holdup, ρ is the phase density and β is the angle of inclination from the horizontal (positive for upward flow). $A'_L = dA_L/dh_L$, where h_L is the liquid level. The subscripts L and G denote liquid and gas, respectively.

When the RHS of [3] equals zero ($F = 0$) the steady-state solution for the liquid level is obtained. The shear stresses τ_L, τ_G and τ_i are evaluated as follows:

$$\tau_L = f_L \frac{\rho_L U_L^2}{2}, \quad [5]$$

$$\tau_G = f_G \frac{\rho_G U_G^2}{2} \quad [6]$$

and

$$\tau_i = f_i \frac{\rho_G (U_G - U_L) | U_G - U_L |}{2}, \quad [7]$$

where

$$f_L = C_L \left(\frac{D_L U_L}{\nu_L}\right)^{-n}, \quad f_G = C_G \left(\frac{D_G U_G}{\nu_G}\right)^{-m}. \quad [8]$$

D_L and D_G are the hydraulic diameters evaluated in the following manner:

$$D_L = \frac{4A_L}{S_L}, \quad D_G = \frac{4A_G}{S_G + S_i}. \quad [9]$$

The coefficients C_G and C_L equal 0.046 for turbulent flow and 16 for laminar flow, n and m take the values of 0.2 for turbulent flow and 1.0 for laminar flow. The interfacial friction factor was assumed to have a constant value of $f_i = 0.014$, as suggested by Cohen & Hanratty (1968) for stratified wavy flow, or f_G when $f_G > 0.014$.

Taitel & Dukler (1976) showed that all the terms in F can be expressed as a function of the liquid level. They further expressed the dimensionless liquid level h_L/D as a function of only two dimensionless parameters. The Lockhart–Martinelli parameter

$$X = \frac{\left(\frac{dP}{dx}\right)_{LS}}{\left(\frac{dP}{dx}\right)_{GS}} \qquad [10]$$

and an inclination parameter

$$Y = \frac{(\rho_L - \rho_G) g \sin\beta}{\left|\left(\frac{dP}{dx}\right)_{GS}\right|}, \qquad [11]$$

where dP/dx is the axial pressure drop and the subscript S is for "superficial".

The dependence of h_L/D on X and Y is shown in figure 1 (Taitel & Dukler 1976; Barnea 1987). It can be clearly seen that for $Y = 4$ and 5 multiple solutions for h_L/D exist. Although the range of parameters of Y for which multiple solutions exist is quite narrow it may be just the actual range in practice (Baker & Gravestock 1987). In figures 2–4 the solutions for h_L/D are presented in dimensional coordinates for an upward inclination angle of 1°. It can be seen that multiple solutions are obtained for a wide range of liquid flow rates and a narrow range of gas flow rates.

When multiple solutions occur, the question of interest is which of these steady states are realized physically and will actually occur.

A very similar problem has been shown to exist in annular flow. Barnea & Taitel (1989) showed that the two-fluid model may yield multiple solutions for the average film thickness in steady annular flow. The differential form of the two-fluid model for annular flow (neglecting surface tension) is ill-posed and a linear stability analysis of annular flow using the two-fluid model and taking the shear stresses into account shows, as is well known, that the steady-state solutions are always unstable due to the K–H type instability (Barnea & Taitel 1989). It has been shown (Andreussi *et al.* 1985; Barnea 1991a) that this instability (the "viscous K–H instability") is related to the instability of the interface resulting in large-amplitude roll waves. Thus, this kind of instability is not appropriate to address the question of which of the steady-state solutions is a stable structure with respect to the average film thickness.

Barnea & Taitel (1989, 1990) suggested a simplified formulation where a uniform film thickness is assumed along the pipe. It has been shown that a stability analysis on this simplified formulation provides the desired answer as to whether annular flow with an unstable wavy interface is a stable structure which can be realized physically. Recently, Barnea (1991b) examined the stability of the structure of annular flow by using the discrete form of the two-fluid model and obtained the same stability criteria as that obtained by Barnea & Taitel (1989, 1990), for a uniform averaged film.

Considering now the stability of the multiple steady-state solutions for stratified flow, one faces similar problems to those described above. A linear stability analysis using the full two-fluid model [1]–[4] yields the following criterion for the stability of the steady-state solutions in stratified flow (Barnea 1991a):

$$(C_V - C_{IV})^2 + \frac{\rho_L \rho_G}{\rho^2 R_L R_G}(U_G - U_L)^2 - \frac{\rho_L - \rho_G}{\rho} g \cos\beta \frac{A}{A'_L} < 0, \qquad [12]$$

where

$$\rho = \frac{\rho_L}{R_L} + \frac{\rho_G}{R_G}.$$

C_V is the critical wave velocity on the inception of instability:

$$C_V = \frac{\left(\frac{\partial F}{\partial R_L}\right)_{U_{LS}, U_{GS}}}{\left[\left(\frac{\partial F}{\partial U_{GS}}\right)_{U_{LS}, R_L} - \left(\frac{\partial F}{\partial U_{LS}}\right)_{U_{GS}, R_L}\right]} \qquad [13]$$

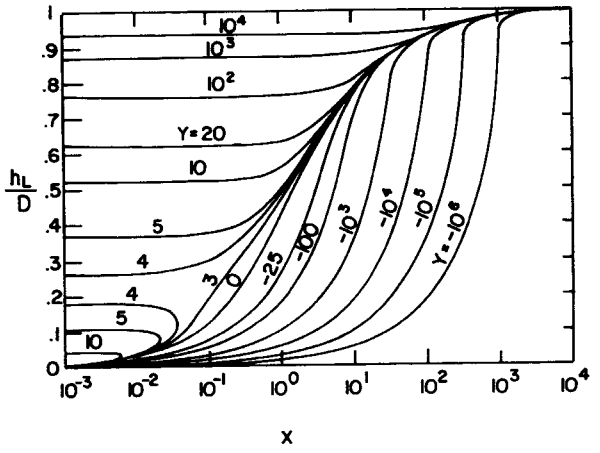

Figure 1. Equilibrium liquid level in stratified flow. Turbulent liquid–turbulent gas.

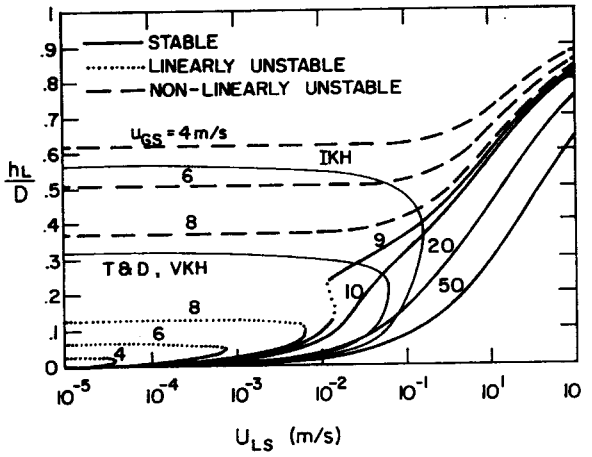

Figure 2. Multiple solutions and structural stability of stratified flow. Air–water, $\beta = 1°$, 0.1 MPa, 25°C, 5.0 cm dia.

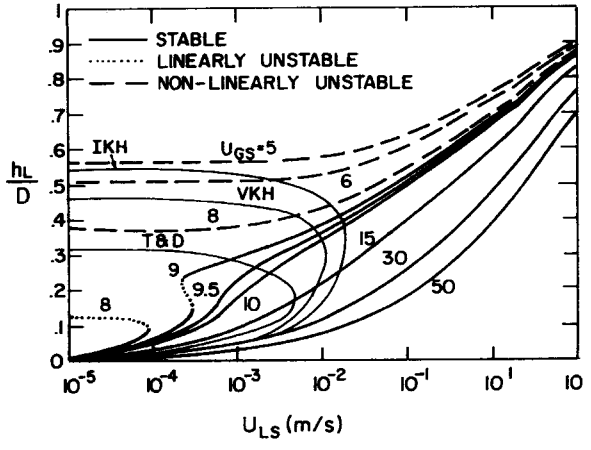

Figure 3. Multiple solutions and structural stability of stratified flow. Air–liquid (μ_L = 100 cP), $\beta = 1°$, 0.1 MPa, 25°C, 5.0 cm dia.

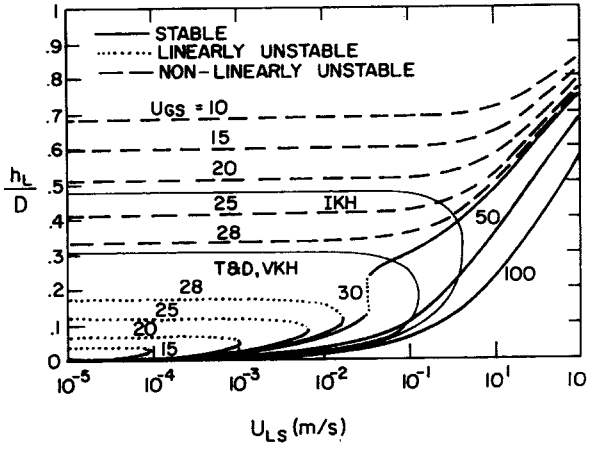

Figure 4. Multiple solutions and structural stability of stratified flow. Air–liquid (μ_L = 100 cP). $\beta = 1°$, 0.1 MPa, 25°C, 50 cm dia.

and

$$C_{IV} = \frac{\rho_L U_L R_G + \rho_G U_G R_L}{\rho_L R_G + \rho_G R_L}. \quad [14]$$

As has been mentioned (Andreussi *et al.* 1985; Barnea 1991a) this criterion [12] is related to the interfacial instability and indicates the appearance of large-amplitude roll waves. However, in order to examine whether the steady-state solution for stratified flow is physically stable with respect to its average film thickness, even when the interface is unstable due to K–H instability, the approach taken for annular flow is also used here.

A hypothetical mechanism that causes the liquid level to be uniform along the pipe of length l is assumed and a quasi-steady-state is considered for the gas phase. Transient momentum and continuity equations are obtained for the liquid phase:

$$\frac{dU_L}{dt} = -\frac{U_{LS}}{R_L l}\left(U_L - \frac{U_{LS}}{R_L}\right) - \frac{F}{\rho_L} \quad [15]$$

and

$$\frac{dR_L}{dt} = \frac{1}{l}(U_{LS} - U_L R_L), \quad [16]$$

where F is given by [4].

A linear stability analysis on the above two ordinary differential equations yields the following criterion for the structural stability of cocurrent stratified flow:

$$\left(\frac{\partial F}{\partial R_L}\right)_{U_{LS},U_{GS}} > 0. \quad [17]$$

Barnea (1991b) showed that this same criterion is equivalent to the requirement that the continuity waves will propagate in the downstream direction, namely that

$$C_K = \left.\frac{\partial U_{LS}}{\partial R_L}\right|_{U_{GS}+U_{LS}} = \frac{\left(\frac{\partial F}{\partial R_L}\right)_{U_{LS},U_{GS}}}{\left[\left(\frac{\partial F}{\partial U_{GS}}\right)_{U_{LS},R_L} - \left(\frac{\partial F}{\partial U_{LS}}\right)_{U_{GS},R_L}\right]} > 0. \quad [18]$$

Based on [4] it can be observed that F always increases with U_{GS} for constant U_{LS} and R_L and decreases with U_{LS} for constant U_{GS} and R_L. Therefore the denominator in [18] is always positive and thus the stability criterion in [18] reduces to [17]. Note that the expression for the kinematic wave velocity, C_K, is equal to the critical K–H wave velocity, C_V [13].

Figure 5 shows the function F vs h_L/D for a specific set of conditions. The zero values of F (the intersection with the broken line) yield the steady-state solutions. As can be seen for $U_{GS} = 8$ m/s three steady-state solutions exist. For $U_{GS} > 8$ m/s a single solution with a low liquid level is obtained, while for $U_{GS} < 8$ m/s a single value that corresponds to a high liquid level is obtained. The stability criterion [17] can be easily applied by observing the slope of the function F vs h_L/D. Thus, when three steady-state solutions are obtained the first solution (the smallest h_L) and the third solution (the largest h_L) are linearly stable with respect to the structure, while the middle solution is unstable and therefore would not exist. Note that a single solution, thin or thick, is always linearly stable.

More information on the steady-state solutions are plotted in figures 2–4 for selected sets of conditions, where h_L/D vs U_{LS} is plotted for different values of the gas flow rates. In these figures the linearly unstable solutions are plotted as a dotted line.

Structural non-linear stability

As mentioned above, when three steady-state solutions are obtained the first (thin) and the third (thick) solutions are linearly stable. The third solution, however, can be unstable to large disturbances and as a result would not exist. The analysis of this kind of non-linear instability is examined by a numerical simulation using the simplified transient formulation, presented as [15]

and [16], that was used to analyze the linear structural stability. Numerical runs were carried out around the three steady-state points obtained, and the path on a phase diagram was observed.

An example of such a transient numerical simulation, for the case $U_{LS} = 0.001$ m/s and $U_{GS} = 8$ m/s, is shown in figure 6, where the trajectories of the transient simulation are plotted on a phase space of U_L vs R_L. The transient simulation starts with conditions close to the linearly unstable solution ($U_L = 0.0135$ m/s and $R_L = 0.0743$). As seen, when we start at a point somewhat to the left of the unstable solution B, we end up with the stable "thin" solution A ($U_L = 0.1578$ m/s and $R_L = 0.00634$). Starting at a point to the right of the unstable solution yields a trajectory that ends up eventually at the stable thick solution C ($U_L = 0.003$ m/s and $R_L = 0.337$), but the trajectory is in the form of severe oscillations before the point of steady state is reached. We consider the third solution as unstable because the trajectory passes through negative liquid velocities. When the liquid velocity becomes negative the structure of co-current flow is destroyed and the transition to slug flow will ensue (Barnea & Taitel 1990). This negative value of U_L is obtained also when the starting point is quite close to the third solution.

In order for a steady-state solution to be stable, it is required that all trajectories will end up at the steady-state point without passing through negative liquid velocities during the dynamic response. It is not practical to determine this non-linear stability condition by checking the dynamic response of all possible disturbances. A way out of solving this problem is as follows: If the RHS of the momentum equation [15] and the continuity equation [16] are plotted on a phase diagram of U_L vs R_L the intersections of these curves yield the steady-state solutions. Figure 7 shows this phase diagram for different values of the pipe length. The dashed line, [16], is always positive while the solid lines [15], may have negative values for the liquid velocities. As can be seen, the lowest values of the liquid velocities are obtained for the limiting case of $l \to \infty$. It is interesting to observe that the transient simulation follows approximately the momentum curve (the solid line) for long pipes (large l), while for short pipes it follows the continuity curve (the dashed line). When the pipe length approaches ∞ ($l \to \infty$) and the momentum line does not pass through negative liquid velocities, then stability to finite disturbances is insured for all cases. Thus, it may serve as a criterion for insuring stability to finite disturbances. Obviously this is not the condition for the case in figures 6 and 7, where the third solution is clearly an unstable structure.

Following this criterion for non-linear stability all unstable cases in figures 2–4 are plotted as a dashed line. As seen, the third of the three steady-state solutions (the thick liquid level) is almost always unstable. But, also when a single solution, which corresponds to a thick film thickness, is obtained, the solution may be unstable to finite disturbances. This can be demonstrated by figure 5. For $U_{GS} = 9$ m/s we have a single "thin" solution which is stable. For $U_{GS} = 6$ m/s we have a single "thick" solution which is linearly stable but unstable due to this non-linear criterion.

In figures 2–4 the stable solutions for the liquid level are plotted as solid lines, the linearly unstable solutions as dotted lines and the non-linear unstable solutions as dashed lines. Usually, when we have three solutions the thinnest solution is stable, the middle solution is linearly unstable and the thickest solution is non-linearly unstable. When a single solution exists, then it is always linearly stable but it may be unstable to finite disturbances, as can be seen, for example, for $U_{GS} < 9$ m/s (figure 2). Note that for $U_{GS} > 9$ m/s the solutions are always stable.

In looking for the possibility of two simultaneous solutions to be structurally stable we can see that this is almost impossible, though it may occur for a very narrow range of gas velocities. For a water–air system (figure 2) only for $U_{GS} \simeq 9$ m/s is it possible to get two stable steady-state solutions for a very narrow range of U_{LS} ($\simeq 0.01$ m/s). The situation is the same for the higher viscous case (figures 3 and 4) were two stable solutions are possible for $U_{GS} \simeq 9$ and $\simeq 30$ m/s, respectively. Thus, although, theoretically multiple solutions may be possible, they are very unlikely to occur in practice.

K–H STABILITY

When stratified flow is structurally stable, steady-state stratified flow is not yet guaranteed and the transition from stratified flow may occur due to K–H interfacial instability. Three types of K–H instabilities were used: simplified K–H stability (Taitel & Dukler 1976); inviscid K–H stability; and viscous K–H stability (Wu *et al.* 1987; Lin & Hanratty 1986).

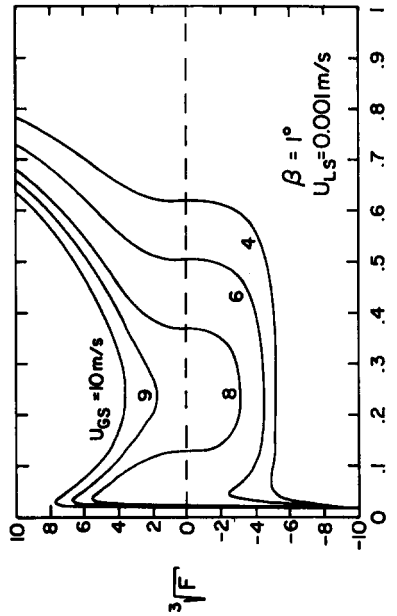

Figure 5. The function F, [4]. Air–water, $\beta = 1°$, 0.1 MPa, 25°C, 5.0 cm dia.

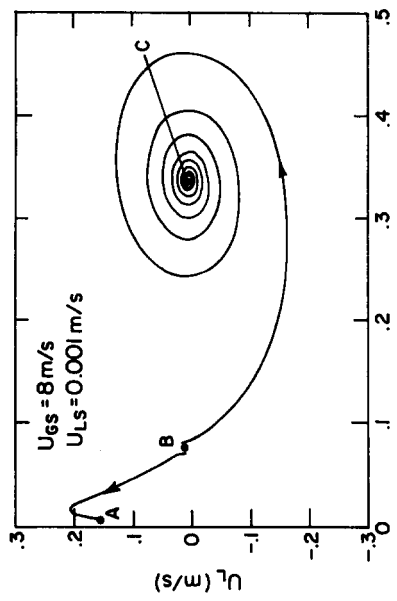

Figure 6. Dynamic simulation, system response to finite disturbance. Air–water, $\beta = 1°$, 0.1 MPa, 25°C, $l = 1$ m, 5.0 cm dia.

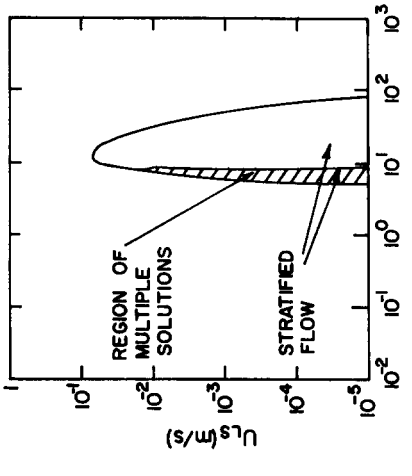

Figure 8. The stratified flow pattern region (using the T&D appraoch) for air–water. $\beta = 1°$, 0.1 MPa, 25°C, 5.0 cm dia.

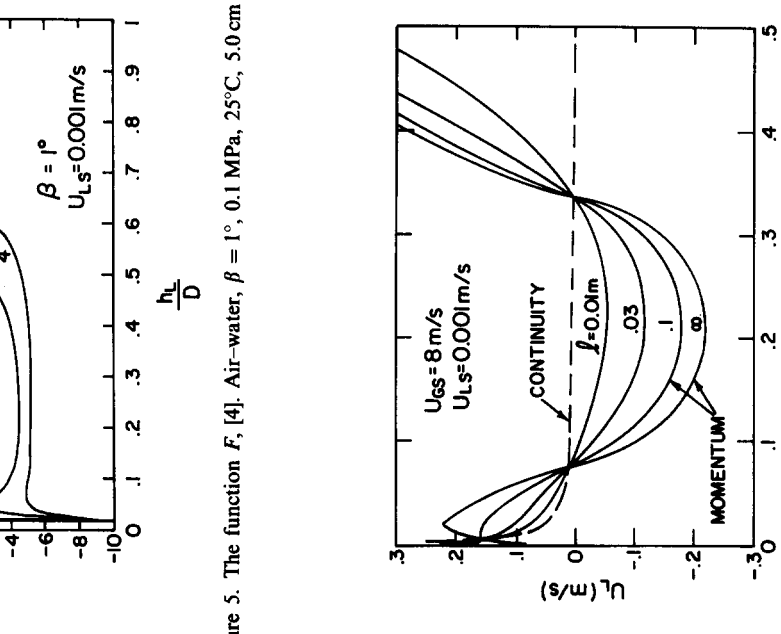

Figure 7. Phase diagram for $U_{LS} = 0.001$ m/s, $U_{GS} = 8$ m/s. Air–water, $\beta = 1°$, 0.1 MPa, 25°C, 5.0 cm dia.

Barnea (1991a) suggested a combined model which uses the viscous and inviscid K–H theories for the determination of the transition from stratified to slug and annular flow. According to this model, the stability condition obtained by the viscous K–H analysis [12] indicates the appearance of large-amplitude roll waves on the interface. For the case of high liquid holdup ($h_L/D > 0.5$) this unstable wave region becomes slug flow. The inviscid K–H analysis, on the other hand, results in an unbounded exponential growth of the waves and designates an absolute transition from stratified flow. Thus, the neutral stability condition obtained by the inviscid analysis demarcates between annular flow and roll waves, within the high void region. Barnea (1991a) also showed that the simplified K–H analysis, suggested by Taitel & Dukler (1976) is fairly consistent with the aforementioned combined method, provided the liquid viscosity is not too large ($\mu_L < 100$).

The stable solutions due to the K–H analyses are also shown in figures 2–4. Three lines of neutral stability are plotted in these figures: (1) the Taitel & Dukler approximate approach (designated T&D); (2) the viscous K–H stability (designated VKH); and (3) the inviscid K–H stability line (designated IKH). Note that in figures 2 and 4 the T&D and VKH neutral stability lines practically overlap. The theory of Taitel & Dukler (1976) suggests that the region within the neutral boundary is stratified (smooth and wavy). Based on more accurate considerations, Barnea (1991a) suggested that the region within the VKH line is stratified smooth or wavy with small amplitude, the region outside the IKH line is non-stratified (slug or annular) and the region between the VKH and IKH lines is stratified with roll waves for $h_L/D < 0.5$ and slug for $h_L/D > 0.5$. Thus, figures 2–4 can serve also as flow pattern maps. Furthermore, they may indicate the possible flow pattern for all the steady-state solutions.

It is important to mention that in previous work, K–H analysis was always applied to the first solution only, i.e. to the solution with the thinnest liquid level. As an example, figure 8 shows the stratified/non-stratified transition, as suggested by Taitel & Dukler (1976), based on the first steady-state solution. Within this stratified region there is only a small subregion where multiple solutions exist. However, only the first solution is physically realistic, since the second intermediate solution is structurally linearly unstable and the third (thick) solution is structurally unstable due to non-linear instability. Note also, that the third solution is usually also unstable to K–H instability. Landman (1991a,b) did not consider the structural stability and obtained that the intermediate solution may exist.

THE COMBINED STRUCTURAL AND K–H STABILITY ANALYSES

In order to examine the existence of stratified flow solutions one should consider both the structural stability of the solution as well as one of the stratified/non-stratified transition criteria which are based on the K–H instability.

Figures 2–4 present the complete information which is necessary to make the decision as to which of the multiple steady-state solutions for stratified flow will actually occur. In figures 2–4 the multiple solutions for h_L/D are presented as well as the various kinds of instabilities. The structural instability is indicated by the dotted (for the linear case) and the dashed lines (for the non-linear instability). The regions that include the stable solutions for the various types of K–H stability (T&D, VKH and IKH) are also shown in these figures.

For example, in figure 2 one can see that within the region bounded by the T&D transition criterion, multiple solutions almost do not exist since only the first solution is structurally stable. The only exception is observed for $U_{GS} = 9$ m/s and a very narrow range of liquid flow rates, where two simultaneous solutions may be structurally stable. Thus, theoretically, hysteresis can occur at a very narrow region of $U_{GS} \simeq 9$ m/s and $U_{LS} \simeq 0.1$ m/s. This precise occurrence, however, is very unlikely.

Based on Barnea's (1991a) approach for the stratified/non-stratified transition criterion, the region bounded by the VKH stability curve is stratified smooth or stratified with small-amplitude waves, while the region bounded between the VKH, and IKH and the $h_L/D = 0.5$ curves indicates the existence of stratified flow with large-amplitude waves. However, all the solutions that are structurally unstable and bounded within the abovementioned region will not occur in practice. For example, the solutions along $U_{GS} = 8$ m/s, which are bounded between the VKH, the IKH and

$h_L/D < 0.5$ curves, are structurally unstable and will not exist; while solutions along $U_{GS} = 9$, 10 and 20 m/s, which are bounded in this region, are structurally stable and will result in stratified flow with high-amplitude waves.

Very similar results are obtained for a liquid viscosity of 100 cP, as indicated by figure 3 (for higher viscosities we do not have multiple solutions), and for larger pipe diameters and high viscosity (figure 4). As can be seen, the possibility of hysteresis occurs again—at $U_{GS} = 9$ m/s for the case shown in figure 3 and at 30 m/s for the case shown in figure 4.

Based on the results of the cases examined it seems that when three solutions do exist it is sufficient to check only the thin solution for K–H stability in order to determine whether the flow will be stratified. The other two solutions are always structurally unstable and thus need not be examined. This general statement could, however, be adopted with caution since it is possible that it does not apply for all operating conditions.

SUMMARY AND CONCLUSIONS

The calculation of the liquid level in upwards stratified flow can lead to multiple solutions and the question of interest is which solution is realistic and will actually exist.

The validity of the solutions is analyzed by examining the stability of the steady-state solutions. Two types of instability are considered: (1) structural instability (linear and non-linear); and (2) K–H instability (which consists of the T&D simplified approach and the combined VKH and IKH analyses). When a steady-state solution is unstable with respect to either of the aforementioned instabilities, this solution will not exist.

An outline of the conclusions is as follows:

(1) Multiple solutions for upwards inclined stratified flow occur at low liquid flow rates and a narrow range of gas flow rates.
(2) When multiple solutions occur we have three solutions for the liquid level. The thinnest solution is the one that is always stable. The middle solution is always linearly structurally unstable and the thickest solution is almost always unstable both to structural and K–H instability, indicating that it would not exist.
(3) The possibility of hysteresis, namely the possible existence of two liquid levels for the same operating conditions, is very unlikely. For all the examples tested we observed only an extremely narrow region for which this can happen (see figures 2 and 3 for $U_{LS} = 9$ m/s and figure 4 for $U_{LS} = 30$ m/s).

REFERENCES

ANDREUSSI, P., ASALI, J. C. & HANRATTY, T. J. 1985 Initiation of roll waves in gas–liquid flows. *AIChE Jl* **31,** 119–126.

BAKER, A. & GRAVESTOCK, N. 1987 New correlations for predicting pressure loss and holdup in gas/condensate pipelines. In *Proc. 3rd Int. Conf. on Multiphase Flow*, The Hague, The Netherlands, pp. 417–435.

BARNEA, D. 1987 A unified model for prediction flow pattern transitions in the whole range of pipe inclination. *Int. J. Multiphase Flow* **13,** 1–12.

BARNEA, D. 1991a On the effect of viscosity on stability of stratified gas liquid flow—application to flow pattern transition at various pipe inclinations. *Chem. Engng Sci.* **46,** 2123–2131.

BARNEA, D. 1991b Stability analysis of annular flow structure, using a discrete form of the "two-fluid model". *Int. J. Multiphase Flow* **17,** 705–716.

BARNEA, D. & TAITEL, Y. 1989 Transient formulations modes and stability of steady state annular flow. *Chem. Engng Sci.* **44,** 325–332.

BARNEA, D. & TAITEL, Y. 1990 Non-linear stability and dynamic simulation of annular flow. *Chem. Engng Sci.* **45,** 3367–3371.

COHEN, & HANRATTY, T. J. 1968.

COHEN, S. L. & HANRATTY, T. J. 1968 Effects of waves at a gas–liquid interface on a turbulent air flow, *J. Fluid Mech.* **31,** 467–469.

LANDMAN, M. J. 1991a Hysteresis of holdup and pressure drop in simulations of two-phase stratified inclined pipe flow. In *Proc. 5th Int. Conf. on Multiphase Production* (Edited by BURNS, A. P.), pp. 19–21. Elsevier, Barking, U.K.

LANDMAN, M. J. 1991b Non-unique holdup and pressure drop in two-phase stratified inclined pipe flow. *Int. J. Multiphase Flow* **17,** 377–394.

LIN, P. Y. & HANRATTY, T. J. 1986 Prediction of the initiation of slugs with linear stability theory. *Int. J. Multiphase Flow* **12,** 79–98.

TAITEL, Y. 1990 Flow pattern transition in two phase flow. Keynote lecture. In *Proc. 9th Int. Heat Transfer Conf.*, Jerusalem, Israel, Vol. 1, pp. 237–254.

TAITEL, Y. & DUKLER, A. E. 1976 A model for prediction of flow regime transitions in horiziontal and near horizontal gas–liquid flow. *AIChE Jl* **22,** 47–55.

WALLIS, G. B. 1969 *One Dimensional Two-phase Flow.* McGraw-Hill, New York.

WU, H. L., POTS, B. F. M., HOLLENBERG, J. F. & MEERHOFF, R. 1987 Flow pattern transitions in two-phase gas/condensate flow at high pressure in an 8-inch horizontal pipe. In *Proc. 3rd Int. Conf. on Multiphase Flow*, The Hague, The Netherlands, pp. 13–21.